The International Journal of Advanced Manufacturing Technology (2023) 125:5445–5461
https://doi.org/10.1007/s00170-023-11083-z

ORIGINAL ARTICLE

Impact of cooled compressed air and high-speed cutting on the drilling of hybrid composite-metal stacks

Cristiano Devitte[1] · André J. Souza[1] · Heraldo J. Amorim[1]

Received: 21 September 2022 / Accepted: 7 February 2023 / Published online: 16 February 2023

Abstract
Hybrid composite-metal stacks (HCMS) combine metal alloys and composite materials and are used in the manufacturing and maintenance of aircrafts. Drilling is an important manufacturing process necessary for installing rivets in fuselages. This work sought to identify the influence of cooled compressed air and high-speed cutting (HSC) on drilling multi-material joints with different configurations. Among the factors observed are the composite type (carbon- or glass-fiber-reinforced polymer), joint type with 2024 aluminum alloy (simple or composed), presence or absence of cooled air, cutting speed (40 and 220 m/min), and feed rate (0.02 and 0.08 mm/rev) in HCMS drilling. Adjusted delamination factor, hole-wall roughness, hole roundness, and thrust force were evaluated. The combined effect between cutting speed and cooled air did not significantly impact the defects generated, making it possible to use HSC without harming the joint. Cooled air showed a tendency to decrease defects in HCMS drilling.

Keywords Drilling hybrid composite-metal stacks · Cooled compressed air · High-speed cutting · Delamination · Hole quality

1 Introduction

Drilling hybrid composite-metal stacks (HCMS) is challenging due to the fiber delamination, tool damage, and matrix damage caused by the thermal and mechanical characteristics of the machining process [1]. In addition, it is challenging to select cutting parameters to guarantee machining quality and surface integrity for all constituents [1-3]. The most common problems during the drilling process of hybrid materials are damage on the contact surface of the composite resulting from its interaction with chips formed in the machining of aluminum (continuous chips) or titanium (saw-tooth chips). Furthermore, the thrust forces generated during drilling may be able to separate the composite from the metal, contributing to accumulating metallic chips and fiber fragments at the metal-composite interface, in addition to the adhesion of metallic material along the entire cutting edge of the tool [1].

Delamination defects on fiber-reinforced polymers (FRP) directly affect the quality of the assembly of structures and decrease the mechanical performance of the parts, especially when subjected to cyclic loads (fatigue). These defects can be identified in the entrance and exit regions of the cutting tool [4]. Delamination at the hole entrance is mostly related to the pull force exerted on the upper layers of the FRP by the main cutting edges in the vicinities of the tool periphery and by the secondary cutting edges due to the sliding of the first ply up the drill flutes; at the exit, it is mainly attributed to the effect of the thrust force on the lower layers of the laminate [4-9]. Different studies have concluded that the feed rate is the most influential input parameter on the delamination factor [7-14] and thrust force [8-18] for the FRP drilling process. Other studies have reported the influence of the drill (diameter, geometry, and wear) on delamination [2, 7, 8, 10-14, 19, 20] and thrust force [4, 8, 10, 13-17, 19, 20].

Delamination defects on fiber-reinforced polymers (FRP) directly affect the quality of the assembly of

✉ André J. Souza
ajsouza@ufrgs.br

Cristiano Devitte
cristiano.devitte1@gmail.com

Heraldo J. Amorim
amorim@mecanica.ufrgs.br

[1] Laboratory of Automation in Machining (LAUS), Mechanical Engineering Department (DEMEC), Federal University of Rio Grande Do Sul (UFRGS), Porto Alegre, RS, Brazil

structures and decrease the mechanical performance of the parts, especially when subjected to cyclic loads (fatigue). These defects can be identified in the entrance and exit regions of the cutting tool [4]. Delamination at the hole entrance is mostly related to the pull force exerted on the upper layers of the FRP by the main cutting edges in the vicinities of the tool periphery and by the secondary cutting edges due to the sliding of the first ply up the drill flutes; at the exit, it is mainly attributed to the effect of the thrust force on the lower layers of the laminate [4-9]. Different studies have concluded that the feed rate is the most influential input parameter on the delamination factor [7-14] and thrust force [8-18] for the FRP drilling process. Other studies have reported the influence of the drill (diameter, geometry, and wear) on delamination [2, 7, 8, 10-14, 19, 20] and thrust force [4, 8, 10, 13-17, 19, 20].

Crown burrs on metallic plates are produced using drills with a lower point angle, resulting in intense forces and plastic deformation in the central region of the hole. Larger point angles allow better distribution of the forces on the periphery of the holes, producing a total or partial fracture in the area and generating smaller and uniform burrs (more easily removed). If this rupture is partial, hat burr occurs [21, 22]. The evaluation of burrs generated between the input and output surfaces of the plates is essential to determine the occurrence of crushing, a defect where the burrs resulting from the drilling of the metallic plate affect the performance of the fiber-reinforced polymer (FRP) acting as support (backplate). During the drilling of the metallic plate, chips are generated, failures occur in the tool, and burrs are produced at the hole exit. In addition, there is challenging to select cutting parameters and optimized tools to ensure the drilling of holes with high dimensional quality while maintaining the integrity of all constituent materials [10, 23]. Among the consequences of burr formation on the entrance and exit surfaces, plastic deformations depend on the material's ductility and surface heating. These are sources of dimensional errors, interferences, misalignments, and initial crack points [24, 25].

Because of the low thermal conductivity of FRP composites, the hard and abrasive characteristics of the reinforcement material cause greater friction by the tool/part contact, increasing the tool heating (it dissipates around 90% of the heat generated in the machining) and, therefore, the tool wear [20, 26]. The polymer matrix degradation tends to occur between 150 and 250 °C, which makes it essential to reduce the temperature in the cutting region [27-30]. A commonly used device is the Ranque-Hilsch vortex tube, which uses only compressed air separated into two streams of different temperatures: hot air and cold air. Physically, the vortex tube consists of a cylindrical tube into which high-pressure gas enters radially, tangent to the inner face of the tube. Secondary gases leave the vortex tube in axial and opposite or coincident directions, depending on the type of construction used, with reverse temperatures [31].

Although some studies pointed out that cutting speed (v_c) did not influence the quality of the drilled holes, distinct research mentioned that a higher v_c, combined with a low feed rate (f), significantly improved this quality, both in micro- and macro-geometric terms. This effect occurs due to the minor influence of the low f, including lower vibration generation and lower thrust forces. Thus, high-speed cutting (HSC) emerges as a solution for drilling hybrid composite-metal stacks [32]. Using HSC allows greater productivity during the process [7, 33], and its combination with cooled compressed air can bring multiple benefits to the hole quality when applied in multi-material joints.

Considering the hindrances of drilling multi-material stacks, this work aims to identify the effects of cooled air, combined with high-speed drilling, on the drilling process of multi-material joints formed by 2024 aluminum alloy and glass- or carbon-fiber-reinforced polymer (GFRP or CFRP).

2 Materials and methods

In this study, the influence of the cutting conditions, including cutting speed, feed rate, cutting tool; the use of cooled air; and the joint composition on the drilling of multi-material hybrids stacks, was investigated. Figure 1 presents the analyses performed and the different experimental combinations**.** The drilled workpieces were distributed in the following configurations and respective joint thicknesses:

- CP1: GFRP + Al 2124 (5.6 ± 0.2 mm);
- CP2: CFRP + Al 2124 (6.2 ± 0.2 mm);
- CP3: Al 2124 + GFRP + Al 2124 (9.7 ± 0.4 mm);
- CP4: Al 2124 + CFRP + Al 2124 (10.3 ± 0.4 mm).

In order to avoid slipping during positioning and subsequent displacement on the holder, the plates were bonded in their periphery using an ethyl-cyanoacrylate-based Loctite adhesive. After being positioned, the joints are fitted using the screw-fixing system of the plate support. After the machining of each hole (sample), the drilling of the following sample is set, including the assembly of the correct stack (drilling of all samples in each stack was not allowed due to randomization). To guarantee the stiffness during machining, each hole was produced at a 15-mm distance from each neighbor (see Fig. 2b). The fastening system has slots that allow chip flow and do not obstruct the generation of burrs.

In this study, the influences of feed rate, cutting speed, tool type, and cooled compressed air are evaluated for drilling the aforementioned multi-material hybrid stacks. The results include the thrust force during the drilling process, the delamination of the composite plates, the

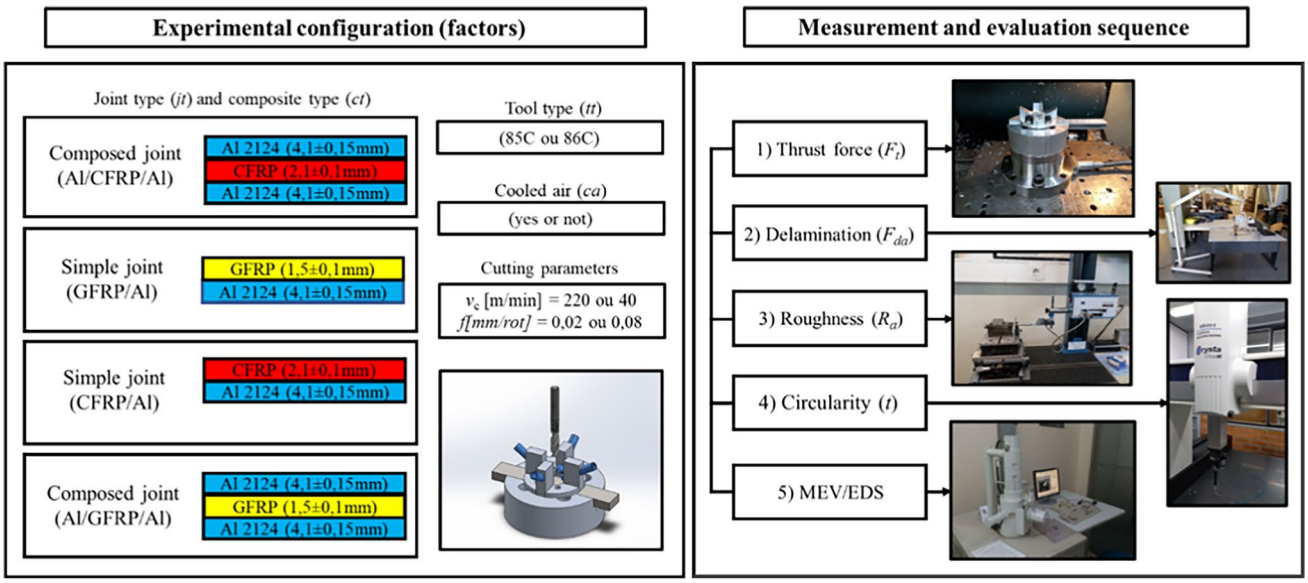

Fig. 1 Experimental combinations and analyses

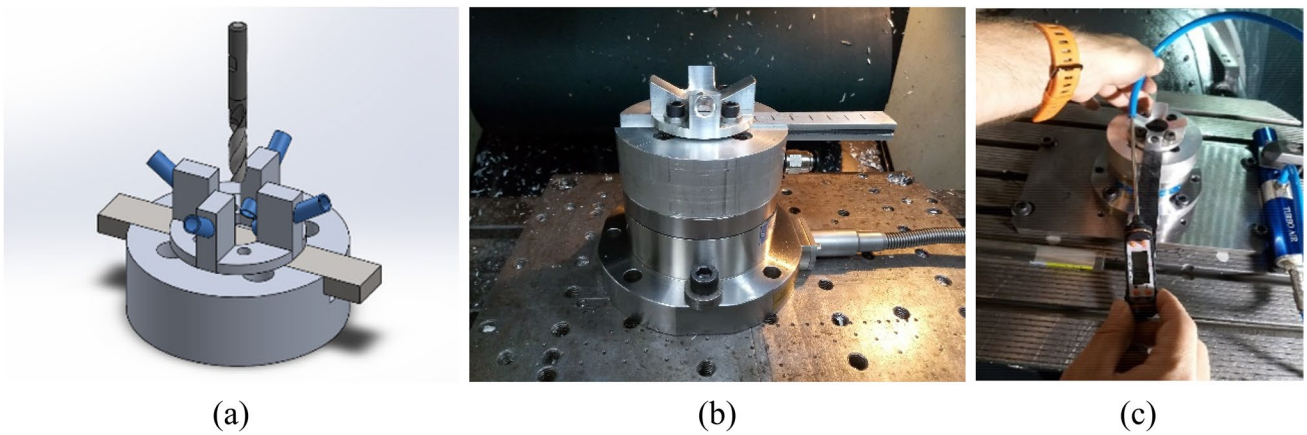

Fig. 2 Workpiece: **a** experimental system assembly for fixing and distributing the cooled compressed air; **b** a set of fixing holes; **c** cooled air temperature measurement system

circularity of the machined holes, and the roughness of the aluminum plates. Scanning electron microscopy (SEM) and energy dispersive spectroscopy (EDS) were also used, as well as X-ray analysis. The levels of the process parameters (factors) used in the experiments are presented in Table 1.

The tests were carried out in a DMG MORI DMU 60 eVo linear universal machining center, with a maximum rotation of 18,000 rpm. The runout was measured at each tool change and remained below 1.3 µm throughout the study. The measurement of thrust force was performed with a Kistler® 9272 stationary piezoelectric dynamometer. The force signals were conditioned by a Kistler® 5070A charge amplifier and acquired by a Measurement Computing® PCIM-DAS 1602/16 data acquisition board. A workpiece-fixturing system was specially developed to position the sample in the dynamometer and distribute the cooled compressed air at

Table 1 Input parameters considered for the study

Parameter	Low level (− 1)	High level (+ 1)
Cutting speed (v_c)	40 m/min	220 m/min
Feed rate (f)	0.02 mm/rev	0.08 mm/rev
Composite type (ct)	GFRP (1.5 ± 0.1 mm)	CFRP (2.1 ± 0.1 mm)
Joint type (jt)	Simple (SJ)	Composed (CJ)
Tool type (tt)	85C ($\sigma = 118°$)	86C ($\sigma = 130°$)
Cooled air (ca)	Yes (Y)	No (N)

the entrance and exit of the hole (Fig. 2a). Figure 2b shows the assembly of the fixturing system in the dynamometer.

Two Sandvik-Precorp uncoated twist drills with split point (cross point) sharpening, helix angle of $\lambda = 27°$, 6-mm diameter, and 110-mm length were used. The Sandvik 85C has a point angle (σ) of 118°, while the 86C drill has $\sigma = 130°$. Cooled compressed air was provided by a Eurotools Turbo Air FTA-12-MC vortex tube. According to the manufacturer, the vortex tube generates a 22.5-m^3/h flow rate with an exit temperature of − 10 °C when supplied by a 6-bar (600 kPa) compressed-air line. However, the cooled-air temperatures, measured before drilling each sample with a portable thermometer (Fig. 2c), varied between 1.8 and 2.2 °C. A cooling time of 120 s was adopted between the drilling of the samples.

The measurement of the hole-wall roughness of the aluminum plates was performed with a Hommel Tester T8000 profilometer equipped with a TkL300 probe with a tip radius of 5 µm and a 90° angle. The hole-wall roughness measurement covered only the metallic plate (aluminum) and used a 0.8-mm sampling length (l_e). Due to the low thickness of the metallic plates (4.1 mm), the maximum evaluation length was $3 \cdot l_e$ (2.4 mm), plus 1.6 mm for the signal filtering [30]. The roughness parameter considered was the average roughness (R_a).

The measurement of the hole roundness deviation was performed on a Mitutoyo Crysta-Plus M7106 coordinate measuring machine (CMM) using the GEOPAK V2.4 R14 software; in this case, eight measuring points distributed along the drilling circumference were considered. The roundness analyses were accomplished at the FRP and metallic plates. The roundness value was considered at the bottom plate metal in the composed joints compared with the aluminum plate in the simple joints. Jointly, scanning electron microscopy (SEM) images of the holes were performed with a Carl Zeiss AG EVO® 50 microscope to identify fractures in the fibers, analyze the surface aspect of the matrix of composites, and examine surface irregularities of holes in the Al 2124 alloy. In addition, elemental chemical microanalysis with energy dispersive spectroscopy (EDS) was performed to characterize the residues observed in the tools.

Contrast radiography was the non-destructive technique chosen to assess the extent of damage in the periphery of the drilled holes. This analysis employed a Kodak 2100 Intraoral X-ray equipment (with a 0.16 s exposure time) associated with the Kodak RVG 5100 digital radiography system and the AnalaR NORMATOR diiodomethane contrast. The acquisition of the images used the Kodak Dental Imaging Software. Finally, the images were processed using the ImageJ public domain software. The use of contrasting liquid is commonly necessary to identify some defects in radiography, such as delamination. The contrast must have a radiopaque character. The parameters of exposure time in the liquid solution and exposure time to X-rays contribute to the final result. The adjusted delamination factor (F_{da}), defined by Eq. (1) [6], was a result of the voids on the surface of the holes observed due to the contrast penetration, where F_d is the ratio between the maximum diameter (D_{max}) of the laminated area and the nominal diameter of the tool (D_o). The composition of defects observed at the hole entrance, exit, and internally was observed by radiography [12].

$$F_{da} = F_d + \left(\frac{A_d}{A_{max} - A_0}\right) \cdot \left(F_d^2 - F_d\right) \quad (1)$$

The design of experiments (DOE) included two tests (T1 and T2) and a fractional factorial (2^{k-1}) with six factors, resulting in 32 holes for each test. Table 2 exhibits the input parameter combinations (cutting conditions) for each drilled hole generated. This experiment used 4-factor and 5-factor interactions for the experimental error term. Combinations of five factors were applied to determine the fractioning of the investigation. The confidence interval adopted was 95%. Factors and interactions with a P-value < 0.05 were considered significant. In addition, considering further analysis in this work, a confidence of 90% was also considered. The experiments were randomized to reduce and minimize the noise levels associated with the investigation. Two holes were performed with each condition tested, totaling 64 holes. The evaluation of the drilled-joint properties with these conditions was carried out to assess the impact of different levels of defects on the mechanical properties.

3 Results and discussions

The analysis of the results focused on evaluating the influence of the different input parameters on the output variables. Thus, the results were divided into thrust force (F_t), delamination, hole-wall roughness, and hole roundness. In addition, the tools used in the experiments were evaluated for possible wear. Lastly, an analysis of the cost associated with the process was performed.

3.1 Thrust force (F_t)

Table 3 presents the P-values obtained by the analysis of variance (ANOVA) for the thrust force (F_t) results. The composite type (*ct*) was the only input factor that did not significantly influence F_t for a 95% confidence interval. According to [4], the mechanical properties of CFRP are generally better than GFRP. However, the resulting thrust force is only 3% higher for CFRP than for GFRP. Among the interaction effects, the significant factors were *jt* x *ca*, *ct* x *ca*, v_c x *tt*, and *ct* x *tt*. The further factors and their interactions were

Table 2 Combinations of input parameters

Drilled holes		v_c (m/min)	f (mm/rev)	*ct*	*jt*	*tt*	*ca*
T1	T2						
1	33	220	0.08	CFRP	SJ	85C	N
2	34	40	0.08	GFRP	CJ	85C	Y
3	35	220	0.02	GFRP	SJ	85C	N
4	36	220	0.08	CFRP	CJ	86C	N
5	37	220	0.08	GFRP	SJ	85C	Y
6	38	40	0.02	CFRP	SJ	86C	Y
7	39	220	0.08	GFRP	CJ	86C	Y
8	40	40	0.08	CFRP	CJ	86C	Y
9	41	40	0.02	GFRP	SJ	85C	Y
10	42	40	0.02	GFRP	SJ	86C	N
11	43	220	0.08	CFRP	SJ	86C	Y
12	44	220	0.02	CFRP	CJ	85C	N
13	45	220	0.02	CFRP	CJ	86C	Y
14	46	220	0.08	GFRP	SJ	86C	N
15	47	40	0.02	CFRP	SJ	85C	N
16	48	40	0.08	CFRP	SJ	86C	N
17	49	40	0.08	GFRP	SJ	86C	Y
18	50	220	0.02	CFRP	SJ	85C	Y
19	51	220	0.02	GFRP	CJ	85C	Y
20	52	40	0.02	GFRP	CJ	86C	Y
21	53	40	0.08	CFRP	CJ	85C	N
22	54	40	0.08	GFRP	CJ	86C	N
23	55	220	0.02	GFRP	SJ	86C	Y
24	56	40	0.08	GFRP	SJ	85C	N
25	57	40	0.08	CFRP	SJ	85C	S
26	58	40	0.02	CFRP	CJ	85C	Y
27	59	220	0.02	GFRP	CJ	86C	N
28	60	40	0.02	CFRP	CJ	86C	N
29	61	220	0.02	CFRP	SJ	86C	N
30	62	40	0.02	GFRP	CJ	85C	N
31	63	220	0.08	GFRP	CJ	85C	N
32	64	220	0.08	CFRP	CJ	85C	Y

Table 3 *P*-values for main and interaction effects by ANOVA of F_t

Main effects	*P*-value	Interaction effects	*P*-value
Feed rate (*f*)	< 0.001	Joint type (*jt*) x cooled air (*ca*)	0.002
Tool type (*tt*)	< 0.001	Composite type (*ct*) x cooled air (*ca*)	0.017
Cooled air (*ca*)	< 0.001	Cutting speed (v_c) x tool type (*tt*)	0.023
Joint type (*jt*)	< 0.001	Composite type (*ct*) x tool type (*tt*)	0.032
Cutting speed (v_c)	0.002	Feed rate (*f*) x composite type (*ct*)	0.057
		Cutting speed (v_c) x feed rate (*f*)	0.092
$R^2 = 98.03\%$			

not influential for the significance level adopted; however, the interaction between the feed rate and composite type (*f* x *ct*) and cutting speed (v_c x *f*) presented significant influence for a confidence interval of 90% (*P*-value < 0.10), thus being considered almost significant. It is worth noting that a determination coefficient (R^2) of 98.03% was observed for the thrust force.

Figure 3 exhibits the main effects of the input parameters, which presented the most significant influence on the thrust force. Feed rate is accepted as the main input

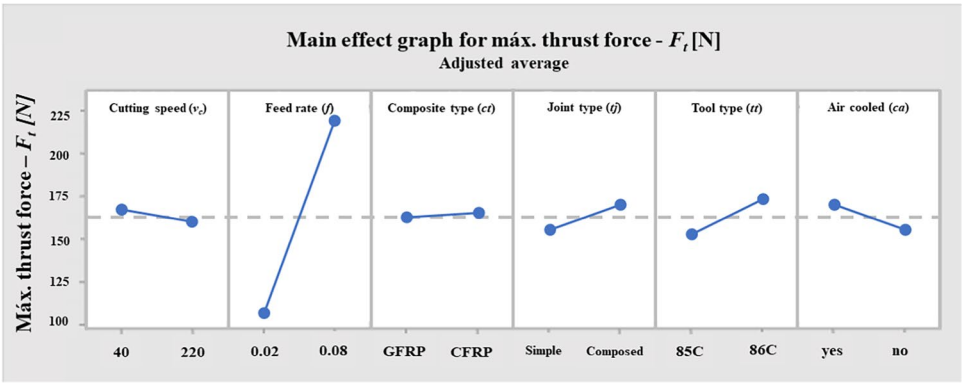

Fig. 3 Main effects for F_t

parameter concerning F_t [12, 13, 15, 18], which was confirmed by the results; in this study, the lowest F_t was observed with the low level of feed rate ($f = 0.02$ mm/rev). The joint type also influenced the mean F_t value due to the increase of the strength resulting from the two layers of metal [34]. The change of the drill point angle affects the contact area during the drilling process, affecting F_t [4, 10, 19] and explaining the low thrust force values observed during drilling with the 85C twist drill. The cooled compressed air (*ca*) favors FRP embrittlement and contributes to chip removal, generating fewer obstacles in the tool feed during the drilling process, which may result in lower F_t [9, 35-37]. However, lower temperatures in the cutting zone may affect the local increase of hardness, especially in metallic plates. The effect of HSC in decreasing F_t was probably related to the lower adhesion of aluminum on the tool edges and surfaces during machining with high cutting speed. With low v_c, the adhesion of aluminum promotes the generation of a built-up edge (BUE), hampering the tool's cutting capacity and contributing to chipping and possible tool failure. BUE was not identified in HSC [38]. The reduction in thrust force (F_t) with a lower feed rate combined with a higher cutting speed was observed by [9] and [18], which agrees with the interaction effect observed for v_c x f, statistically significant for a confidence interval of 90%.

The interaction between joint type and cooled air (*jt* x *ca*) presented a significant influence on the thrust force. In this case, deformations associated with burr generation on the superior metallic plates and with the compressive load of the metallic plates are observed. On the other hand, the use of cooled compressed air contributes to the removal of chips and other residues that would obstruct the movement of the tool [16, 17]. The interaction *ct* x *ca* also was significant for F_t. Besides the effect on the thrust force, it can contribute to reducing composite delamination due to the smaller resilience of the composite resulting from the cooling effect, which improves fiber cutting, making it less susceptible to failures [9, 24, 35, 36]. The interaction v_c x *tt* is associated with the different drill point geometries and cutting speeds and reflects the sum of the thermal effects caused by the input parameters on the properties of the machined materials [14, 19]. Finally, the interaction *ct* x *tt* is influenced by the different critical forces (F_{cr}) that can influence the axial loads, besides the already mentioned influence of the drill point [3, 14].

3.2 Adjusted delamination factor

Table 4 presents the *P*-values of the adjusted delamination factor (F_{da}) from the ANOVA. The main effects, which showed significant influence (*P*-value < 0.05) on the adjusted delamination factor (F_{da}), were joint type (*jt*), composite type (*ct*), and cutting speed (v_c). The determination coefficient calculated for F_{da} was $R^2 = 77.93\%$.

The main effects on the adjusted delamination factor are shown in Fig. 4. The cutting speed was the input parameter, which presented the third most significant influence on F_{da}, with more severe delamination observed after HSC

Table 4 *P*-values for main and interaction effects by ANOVA of F_{da}

Main effects	*P*-value	Interaction effects	*P*-value
Cutting speed (v_c)	< 0.001	Feed rate (*f*) x tool type (*tt*)	0.004
Composite type (*ct*)	< 0.001	Feed rate (*f*) x composite type (*ct*)	0.008
Joint type (*jt*)	< 0.001	Composite type (*ct*) x tool type (*tt*)	0.009
		Composite type (*ct*) x joint type (*jt*)	0.041
		Cutting speed (v_c) x tool type (*tt*)	0.092
$R^2 = 77.93\%$			

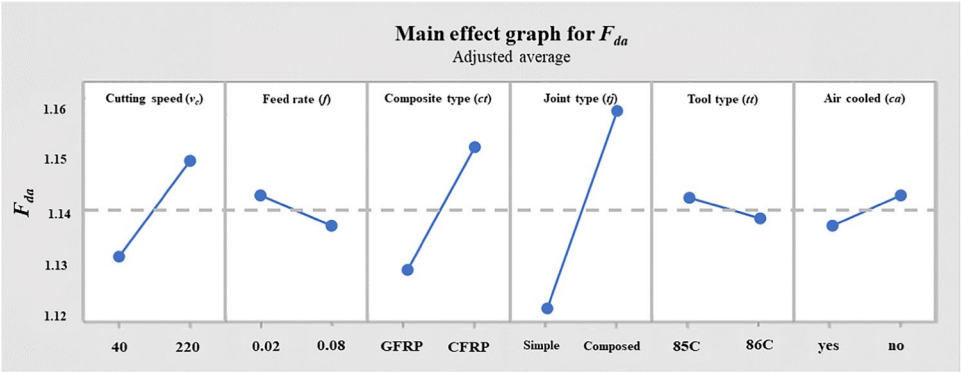

Fig. 4 Main effects for F_{da}

drilling compared with the low level of v_c. This effect is often associated with the higher friction in the tool-FRP interface, which may result in overheating (evidenced by surface burns). Overheating is an undesired effect, especially in the vicinities of the vitrification temperature of the composite matrix, reducing the durability and stability of the stack joint [29, 30]. The composite type (*ct*) also presented a significant influence on the F_{da}: GFRP delamination was significantly lower than that observed in the CFRP plate. This behavior was expected: the strength associated with each composite and their critical forces (F_{cr}) are distinct and may be related to damages [5]. The input parameter, which presented the most significant influence, was the joint type (*jt*). The F_{da} resulting from drilling-composed joints is significantly higher than in simple joints. This difference is associated with the formation of a burr at the exit of the metallic material (Al 2124 alloy) positioned over the composite, which exerts a compressive load on the FRP and increases the delamination.

Despite the smaller values observed with the higher level of this input variable, the feed rate did not present a significant influence on the delamination factor for the tested conditions. This effect was not expected since the thrust force, strongly influenced by *f* in this study, is broadly reported to affect the delamination [8, 10]. From this point of view, higher feed rates would result in higher F_{da} due to the increase of the thrust force with *f* observed in this study [14, 16, 17]. Despite reports of the negative influence of the feed rate in the delamination, this was not observed in this study, where the samples drilled with the highest *f* presented slightly smaller F_{da}. On the other hand, a direct implication of a higher feed rate is the shorter machining time, which tends to reduce the maximum temperature preventing the degradation of the matrix properties and possibly reducing delamination [24, 29, 30]. The explanation for the observed results is the direction of the stack drilling: since the FRP plate was always positioned over a metallic plate, the resulting stiffness prevents the push-out delamination. This effect was also observed by [18].

The influences on F_{da} associated with the tool type (*tt*) (85C and 86C) were not significant for the main effect. Then, regardless of the drill type used, both statistically promote the same level of damage by delamination. The feed rate (*f*) and cooled compressed air (*ca*) did also not demonstrate significant effects; however, higher *f* (0.08 mm/rev) and drilling with cooled air tend to reduce F_{da}.

The ANOVA pointed out some significant interaction effects, including the interaction between the feed rate and tool type (*f* x *tt*), whose main effect on the adjusted delamination factor was also not significant. For the samples machined with the 85C drill, F_{da} increased with feed rate, while the inverse is observed with the 86C drill. These different behaviors can be related to the different drill point angles (118° and 130°), as they cause distinct defects due to the effect of the different cutting thicknesses and to the locking of the FRP plate by the aluminum plate in the HCMS. The different geometries of the cutting tools also affect the thrust forces and their relationship with the feed rate, as demonstrated by [4, 13, 14]. The interaction between feed rate and composite type (*f* x *ct*) is manifested by the increase of F_{da} with *f* in the drilling of CFRP stacks against the decrease of F_{da} when the composite material is GFRP. This effect can be associated with chip formation, resulting in smaller fiber and matrix plucking for GFRP than CFRP [4]. The main explanation for the observed result is the already-mentioned increase in stiffness caused by the lower aluminum plate support. For GFRP, the limit is reached with smaller loads, promoted by the lowest feed rate. The thrust force increases with *f*, and thus F_{da} increases [13].

The tool type is reported to affect the delamination in FRP drilling; this defect can be associated with the drill point angle, making it more susceptible to defects [12-14]. However, no significant influence was observed for the tool type (*tt*) on the adjusted delamination factor, which can also be related to the inhibited push-out delamination due to the support of the lower aluminum plate. Nevertheless, drilling GFRP with the 85C drill results in a lower F_{da} than the 86C drill, while smaller delamination in CFRP drilling is

achieved with the 85C drill. The ANOVA explains this effect by the significant interaction *ct* x *tt*.

The interaction *ct* x *jt* presented a significant influence on the adjusted delamination factor. Drilling of GFRP joints resulted in smaller F_{da} compared with CFRP joints. The highest delamination was observed in holes drilled in composed GFRP joints, while drilling of single GFRP joints resulted in smaller F_{da}. For the reasons mentioned earlier, the highest F_{da} occurred during the machining CFRP in the composite joint due to higher thrust force; on the other hand, the lowest F_{da} occurred when drilling GFRP in the simple joint. Despite the not-significant influence of the interaction *f* x *jt*, an increase of the adjusted delamination factor was observed in the holes drilled with the highest feed rate in the simple joint; on the other hand, F_{da} decreased with the growth of feed rate in the machining of the composed joint. The highest F_{da} value was observed in the holes drilled with $f = 0.02$ mm/rev in the composed joint, possibly due to burr formation, chip flow, and adhesion of aluminum on the tool cutting edges [4, 16, 39].

No significant influence of the use of cooled compressed air or its interactions was identified through the analysis of variance. However, lower delamination was observed in holes drilled with 40 m/min and cooled compressed air. Although not significant, there seems to be a slight tendency to produce holes with smaller F_{da} using cooled air when the lower levels of feed rate and cutting speed are used. This reduction can be related to the thermal effects caused in the composite matrix, which may have improved its integrity and the hole quality at low temperatures, preventing fiber pull-out and contributing to lower delamination [24, 28-30, 37].

According to some studies, cooled air-assisted drilling provides a more regular cutting operation when compared with machining without cooled air. The cooled air probably influenced the temperatures on the tool/composite interface, resulting in better stability of the FRP during the cutting process. The absence of cooled air is reported to increase hole-wall roughness and delamination [24]. In this case, the heat removal effectiveness in drilling (tool, material, and chip) reduces the high-temperature effects on the matrix and fibers [29], thus reducing delamination [28, 37]. The smaller delamination in CFRP drilling with cooled air agrees with the results of [9] and [35]. Hoffmann et al. [37] also observed that drilling with cooled compressed air improves fiber cutting due to its smaller resilience at low temperatures. The cleaner fiber cutting helps prevent the pull-out phenomenon, generating lower roughness values but increasing delamination (fiber pull-out causes high cavities on the surface). Although some of these effects have also been observed in this work, they were not significant.

Figure 5 shows SEM images of holes 43 (simple joint with 86C drill) and 64 (composed joint with 85C drill), with cooled air-assisted drilling, $v_c = 220$ m/min, and $f = 0.08$ mm/rev. No apparent surface defects on CFRP were observed in the SEM analysis of hole 43, and $F_{da} = 1.12$ (Fig. 5a). The hole contour region (Fig. 5b) and the fiber cut (Fig. 5c) are regular. Multiple defects were observed around the surface of hole 64 ($F_{da} = 1.24$), characterized by superficial marks on the CFRP (Fig. 5d) and in the hole border (Fig. 5e), besides irregular fiber and matrix cut (Fig. 5f). Thus, the origins of possible failures were characterized by the fiber rupture and matrix degradation, which can be attributed to the formation of burrs at the exit of the upper aluminum plate and the respective compressive load on the FRP in the composed joints [4, 16, 39]. The plastic deformation caused by the burr formation harms the composite [9, 34], leading to an increase in defects [21-23]. Although the 86C drill tended to reduce F_{da}, this comparison was selected because the tool type (*tt*) was not significant for a 95% confidence interval.

Figure 6 presents SEM images of the exit of hole 03 (GFRP with cooled air) and hole 50 (CFRP without cooled air) after drilling single joints with the 85C drill using HSC and $f = 0.02$ mm/rev. Although cooled air tends to reduce the delamination in drilling with low cutting speed, this comparison was selected due to the non-significant influence of *cc* on the F_{da}. An overview of hole 03 (GFRP with $F_{da} = 1.13$) presents a regular border (Fig. 6a) with no clear push-out defects. Closer inspection indicates a regular cutting; the distinct shape of the fibers in the hole border (Fig. 6b) evidences the clean cut of the glass fibers and the stability of the matrix during the machining of the sample (Fig. 6c). In contrast, the overview of hole 50 (Fig. 6d), with $F_{da} = 1.11$, shows an irregular border, typical of moderate push-out delamination. Despite the more regular border observed in the inner FRP plies (Fig. 6e) when compared with hole 03, there are signs of matrix degradation and a CFRP fiber pull-out (Fig. 6f). The delamination results agree with data presented by other studies [7, 9, 29].

3.3 Hole-wall roughness

Table 5 presents the *P*-value of the main and combined effects on the average roughness (R_a) obtained by ANOVA, with a coefficient of determination (R^2) of 78.31%. The cutting speed (v_c), feed rate (*f*), and tool type were significant for a 95% confidence interval; lower cutting speed, higher feed rate, and the use of the 86C drill ($\sigma = 130°$) are associated with low R_a. Figure 7 presents the SEM analysis of the entrance of hole 59, machined with $v_c = 220$ m/min, and hole 10 ($v_c = 40$ m/min), where the difference between the quality of the holes is clear. The v_c x *f* interaction was significant; higher cutting speed resulted in the increase of the average roughness for both tested feed rates, but with $f = 0.08$ mm/rev, the slope of the R_a x v_c curve was reduced, and a smoother increase was observed. For the interaction

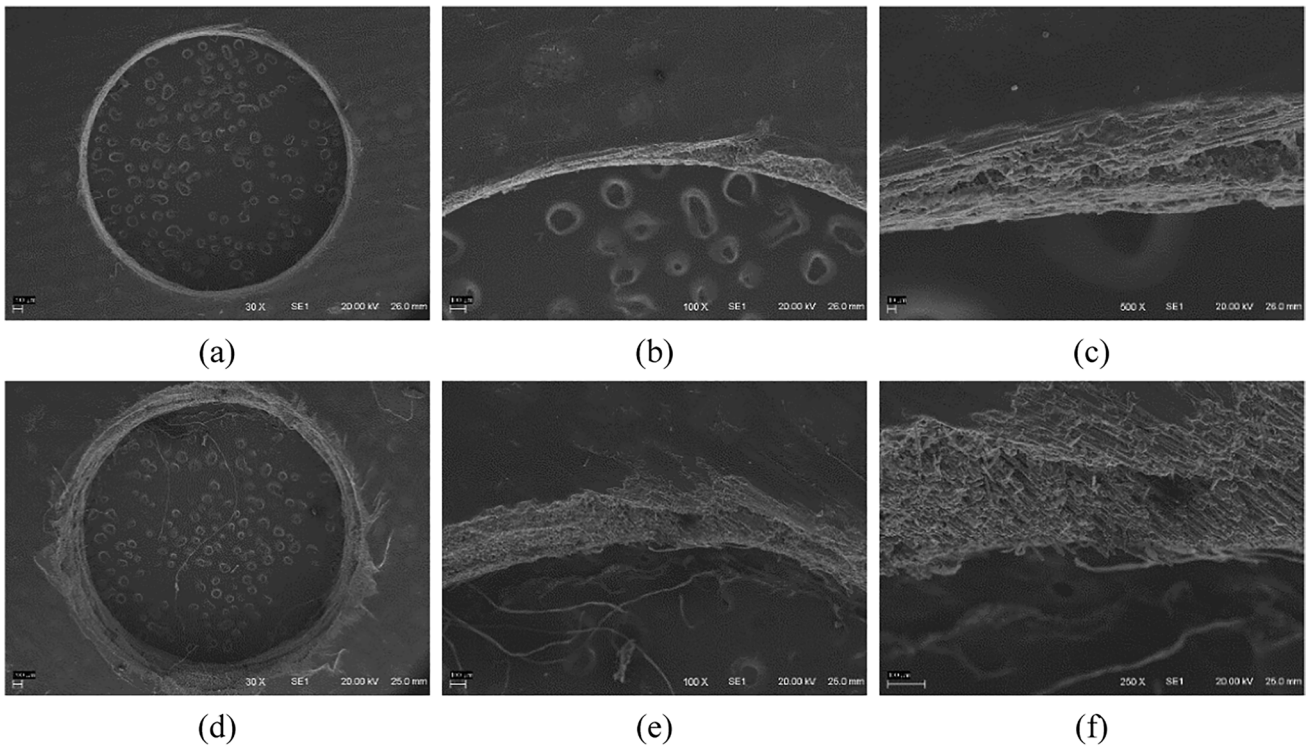

Fig. 5 SEM analysis of the CFRP: composite input (**a**), detail of the hole contour (**b**), and fibers from the region of greatest delamination (**c**) in hole 43; composite input (**d**), detail of the hole contour (**e**), and fibers from the region of greatest delamination (**f**) in hole 64

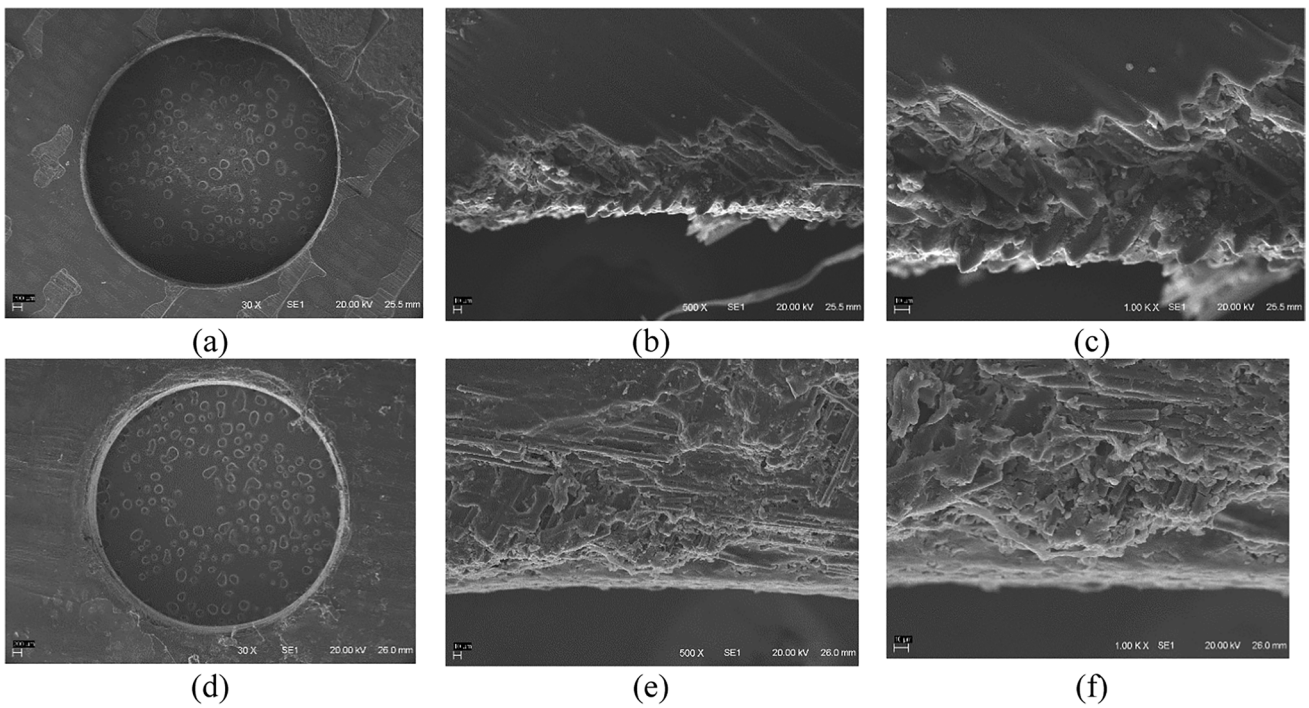

Fig. 6 SEM analysis of GFRP: an overview (**a**) and details of the fibers on the circumference of the hole 03 exit (**b**, **c**). SEM analysis of CFRP: an overview (**d**), details of the fibers on the circumference (**e**), and broken fibers of hole 50 exit (**f**)

Table 5 *P*-values for the main and combined effects for average roughness

Main effects	*P*-value	Interaction effects	*P*-value
Cutting speed (v_c)	< 0.001	Cutting speed (v_c) x feed rate (f)	< 0.001
Feed rate (f)	< 0.001	Cutting speed (v_c) x tool type (tt)	0.002
Tool type (tt)	0.008		
Composite type (ct)	0.099		
Joint type (jt)	0.099		
$R^2 = 78.31\%$			

between v_c and tool type, R_a increased with $v_c = 220$ m/min regardless of the drill type.

The Al 2124 is a ductile aluminum alloy that forms continuous chips while machining. This tendency is potentialized when low feed rates are used. In the drilling process, the removal of the long, continuous chips is often deficient, and these chips may block the helix channels and harm the internal surface finish of the holes. The increase of the cutting thickness favors the formation of shorter chips, which are more easily removed, and can be done by increasing the feed rate and the tool point angle [14]. Higher cutting speeds are usually related to higher temperatures, which favor long and flexible Al chips [30]. Other studies associated high roughness values with tool wear caused by the adhesion (due to aluminum ductility) and abrasion (intensified by the hard fibers of composite) mechanisms [20, 26, 32].

Figure 8 shows the surface characteristics analyzed by SEM of hole 59 ($v_c = 220$ m/min and Al/GFRP/Al joint) and hole 10 ($v_c = 40$ m/min and GFRP/Al joint) at the entrance on the bottom aluminum plate when drilling with 86C tool and $f = 0.02$ mm/rev. Since the joint type was not significant, the comparison between these holes is acceptable. Noticeable differences in surface quality are observed in the analysis of holes 59 and 10: the surface patterns of hole 59 ($R_a = 3.06$ µm), characterized by larger grooves and

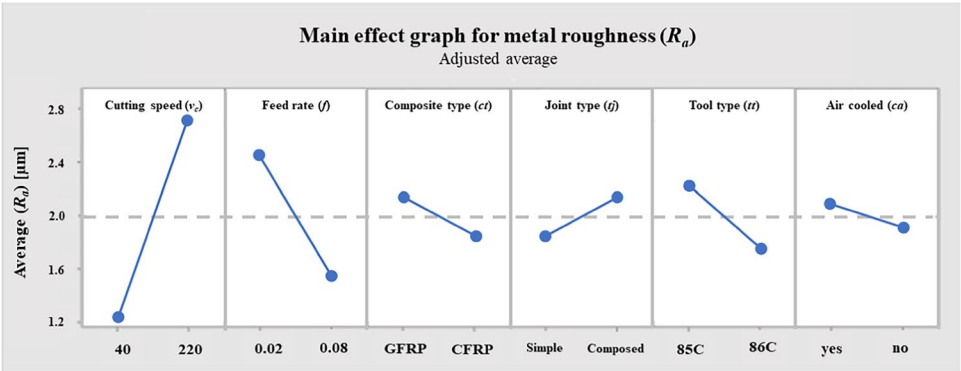

Fig. 7 Main effects for hole wall roughness (R_a)

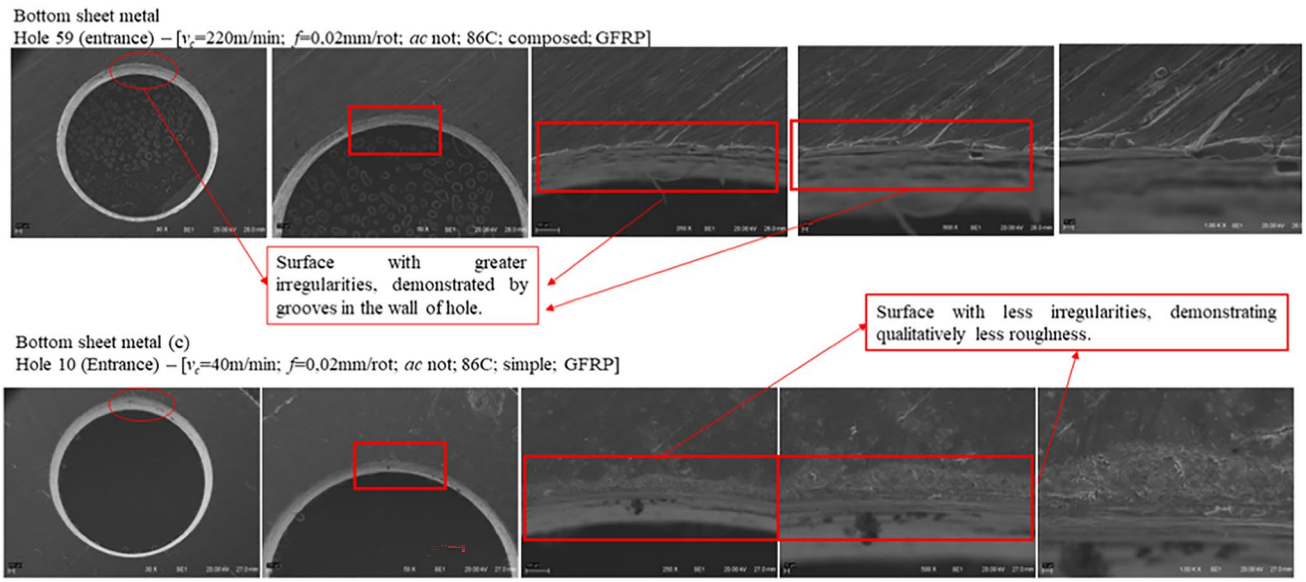

Fig. 8 Comparative SEM analysis of hole wall roughness and irregularities at the entrance of holes 59 and 10 on the aluminum bottom plate

irregular points, can be qualitatively compared with hole 10 ($R_a = 1.59$ µm), which presented a more cohesive and regular surface, in agreement with the respective R_a values. The differences observed in the analysis of both holes are possibly related to the aluminum chip flow due to the different joint types [16, 17].

Since the analysis was conducted in the metallic plate (aluminum), the composite type (*ct*) and the joint type (*jt*) were not expected to influence the hole-wall roughness. Despite the non-significant influence on hole roughness for the 95% confidence interval, the ANOVA indicates that both joint type and composite type present a significant influence for a confidence interval of 90%. Composed joints showed higher roughness values than single joints, probably due to the higher thickness of composed joints, which means longer machined lengths compared with simple joints and, thus, more friction heat generation and higher temperatures since the analysis was performed in the bottom plate [30, 40].

3.4 Hole roundness deviation

Table 6 presents the *P*-values generated by the ANOVA for hole roundness deviation (*t*). For the metallic plate, only the feed rate (*f*) and cutting speed (v_c) presented significant influence with a confidence interval of 90%, and the determination coefficient was 47.94%. In the composite plate, joint type (*jt*), composite type (*ct*), and the combination *jt* x *ct* significantly influenced the hole roundness deviation ($R^2 = 60.44\%$). The non-controllable input parameters could have affected the coefficient of determination (R^2) in the roundness measurement, affecting the results. One of these parameters is the progress of tool wear that, despite being monitored and well above the tool life criteria, might still contribute to this result [20, 26].

Table 6 *P*-values for the main and combined effects for roundness on metallic and composite plates

Metallic plate (t_{metal})		Composite plate (t_{comp})	
Effects	*P*-value	Effects	*P*-value
Cutting speed (v_c)	0.005	Joint type (*jt*)	< 0.001
Feed rate (*f*)	0.038	Composite type (*ct*)	0.011
v_c x *f*	0.085	*jt* x *ct*	0.001
		f x *tt*	0.051
		tt x *ca*	0.067
		f x *ca*	0.084
$R^2 = 47.94\%$		$R^2 = 60.44\%$	

Figure 9 presents the main effects on the roundness deviation in the aluminum holes. The analysis of the significant effects (cutting speed and feed rate) indicates a tendency to increase t_{metal} when the higher cutting speed is used and a decrease with higher *f*. Despite the deviations not exceeding 25 µm, the results indicate that conditions associated with higher heat generation (high v_c, low *f*) are prone to produce holes with larger diameters. This effect is also observed in the absence of cooled compressed air, indicating some influence of the thermal expansion of the aluminum, mitigated when high *f*, low v_c, and *ca* are used [30]. Besides the effects of v_c and *f*, the composite type (*ct*) and cooled air (*ca*) on *t*metal are statistically significant for a 90% confidence interval. The other main factors (joint type and tool type) were not statistically significant for metal roundness deviation and may have contributed to the low R^2.

The main effects on the hole roundness deviation in the composite (*t*,comp) are shown in Fig. 10. The composite type (CFRP promoted an increase of $t_{,comp}$, joint type (composed joint increased the deviation) and their interaction (*ct* x *jt*) significantly influenced the roundness deviation in the composite plate for the 95% confidence interval. For the combined effects, roundness deviation increased for the composed joint (also indicating some influence of thermal expansion), with a more pronounced effect for the CFRP stacks. The smaller deviations identified in the GFRP stacks are corroborated by the cleaner cuts of the fibers (Fig. 6b). The change in the direction of the force applied by the tool after the drilling of the upper plate reduced the cutting stability, contributing to the buckling effects while drilling the composite plate. This effect was not observed in the drilling of simple joints.

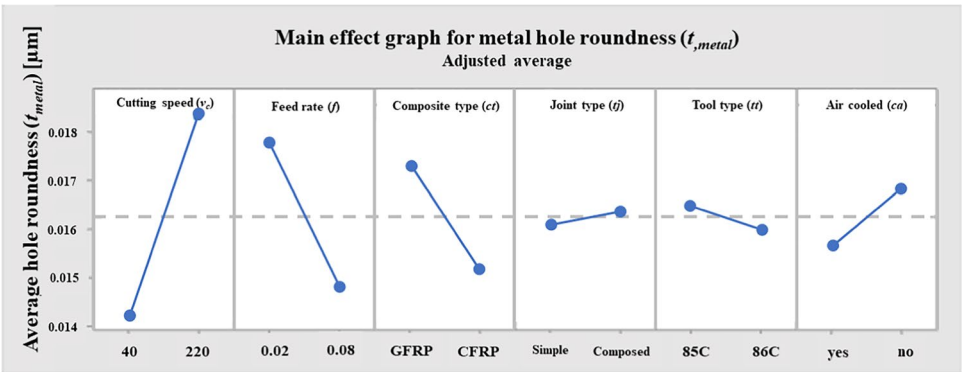

Fig. 9 Main effects for metal hole roundness for t_{metal}

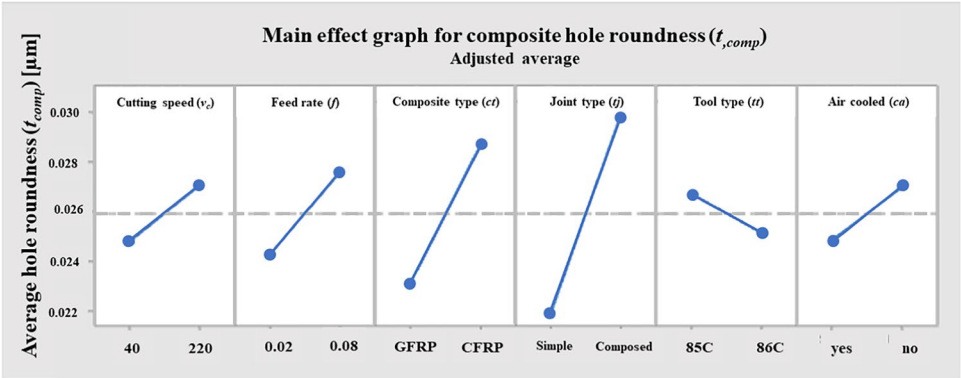

Fig. 10 Main effects for composite hole roundness for t_{comp}

The input factors v_c, f, tool type, and cooled air were not significant for the 95% confidence interval. However, higher roundness deviations (although not exceeding 55 µm) were observed for HSC, even in the presence of cooled air. Both the tool type and cooled compressed air presented significant interactions for a confidence interval of 90%, with the effects of f x ca, f x tt, and tt x ca, showing an almost significant influence on the hole roundness deviation in the composite material. Drilling with the smallest feed rate tested (0.02 mm/rev) produced holes with smaller $t_{,comp}$ when combined with the cooled air, which agrees with reports that link smaller geometric deviation and surface defects to lower temperatures [27]. Finally, the highest t,comp values were achieved with $v_c = 220$ m/min and $f = 0.02$ mm/rev, possibly due to the composite matrix damage caused by the higher friction associated with this combination [30, 33].

3.5 Analysis of the tool condition

Both tool wear and wear types were investigated in this study. Figure 11 presents the SEM analysis of the 85C drill. Intense abrasive wear was observed on the tool corner, and material adhesion was observed on the chisel edge. EDS analysis identified metallic residues, with aluminum being the predominant element (as expected). This adhesion may affect the cutting performance of the tool [20, 26, 39]. SEM/

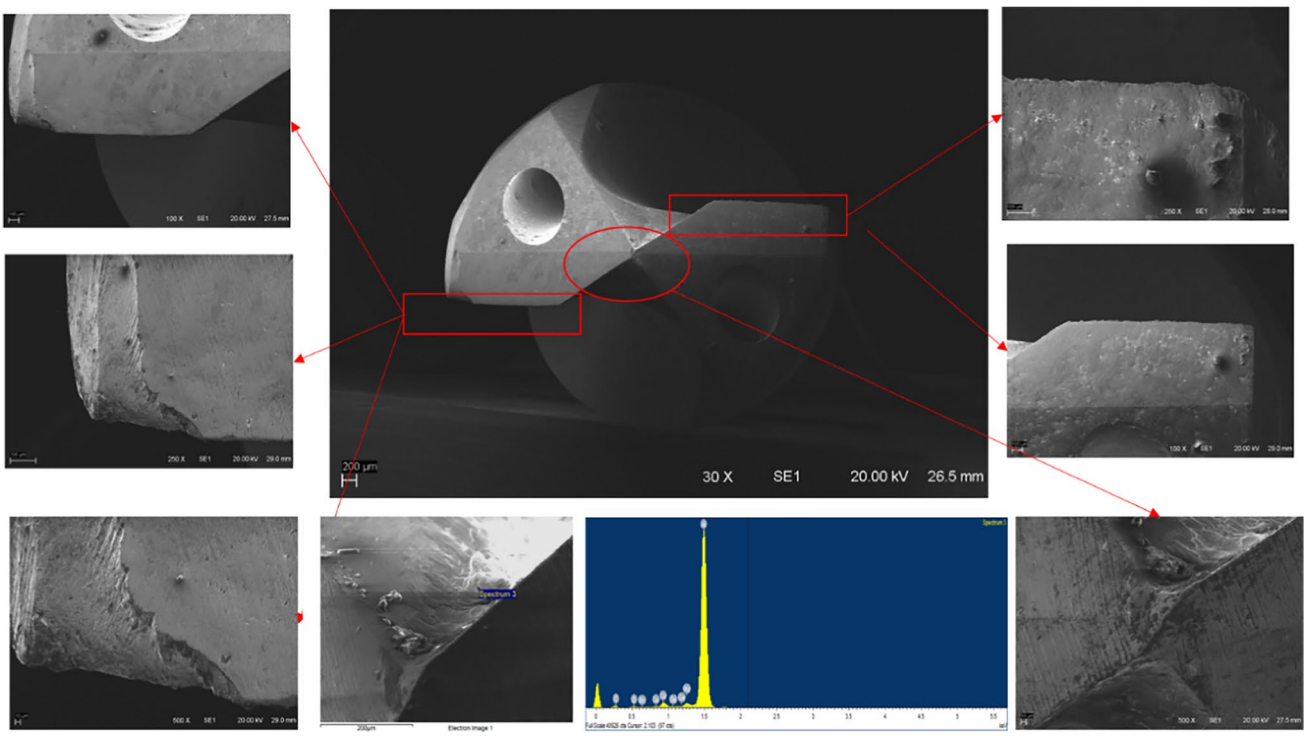

Fig. 11 SEM analysis of 85C drill used in FRP/Al experiments and verification with EDS

EDS analysis of the 86C drill (Fig. 12) shows the adhesion of aluminum on the main cutting edge and the chisel edge, as expected. However, no significant flank wear was observed on the tool edges. Due to the drilling direction from FRP to aluminum, no residues of composite elements were observed in the tested tools [3].

3.6 Additional tests

Additional tests were performed in order to better assess the behavior of the cutting speed and compressed air in more restrictive conditions. Most of the parameters studied in the main study were fixed: tool type (85C), joint type (simple), composite type (GFRP), and feed rate ($f = 0.02$ mm/rev). This resulted in a 2^k factorial DOE with two controllable factors, totaling four distinct conditions: $v_c = 220$ m/min without cooled air (OTM 1), $v_c = 220$ m/min with cooled air (OTM 2), $v_c = 40$ m/min with cooled air (OTM 3), and $v_c = 40$ m/min without cooled air (OTM 4). Three holes were drilled for each condition, i.e., holes #1 to #3 (OTM 1), holes #4 to #6 (OTM 2), holes #7 to #9 (OTM 3), and holes #10 to #12 (OTM 4). The response variables evaluated were maximum thrust force (F_t), the adjusted delamination factor (F_{da}) at the GFRP hole, hole-wall roughness (R_a), and roundness deviation (t_{metal}) at the Al 2124 hole. Table 7 presents the average results for each condition. The thrust force (F_t) did not show wide variation for the different conditions. This was expected due to the fixed feed rate since this parameter significantly affects F_t, and tool geometry remained constant. However, slightly higher F_t values were observed with cooled air (OTM 2 and OTM 3) for both cutting speeds tested. This effect can be attributed to compressed air producing axial and radial loads during the drilling process [35]. This lower temperature influence on Al 2124 enhances the machining difficulty, increasing the forces associated with the drilling process. This effect was also observed in

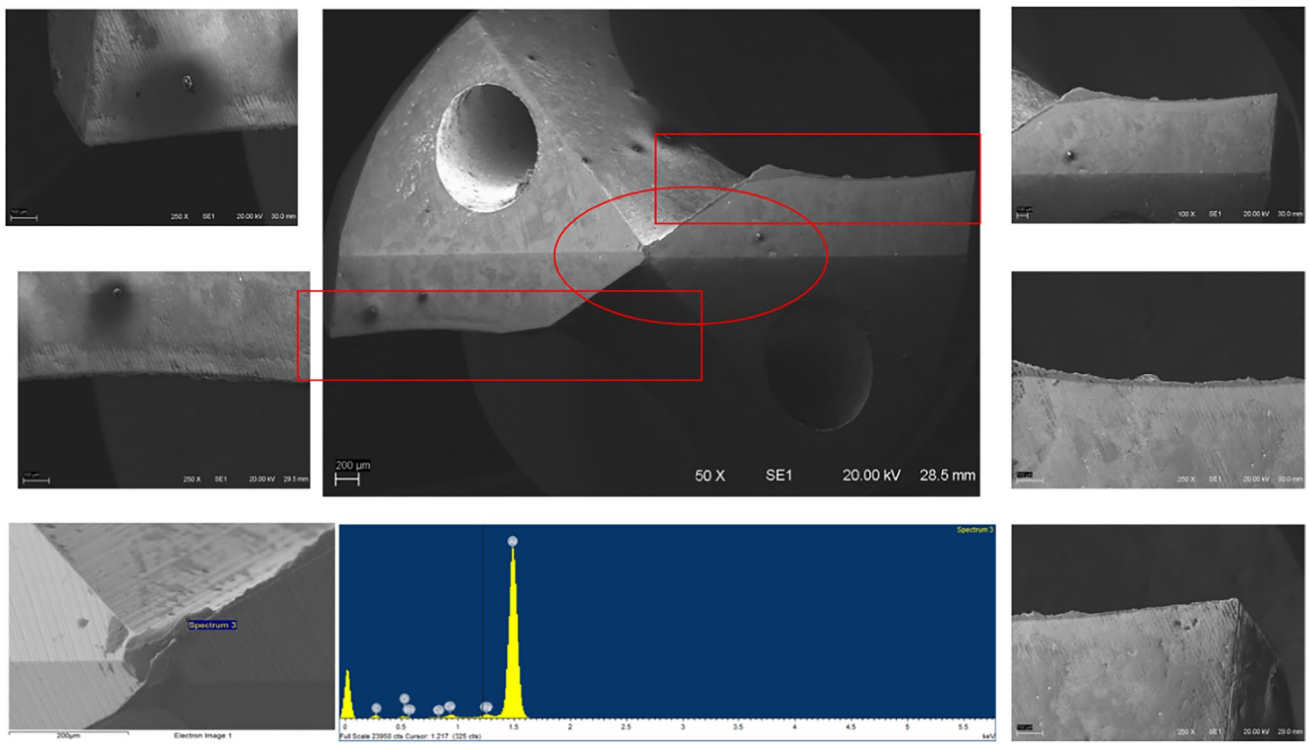

Fig. 12 SEM analysis of 86C drill used in FRP/Al experiments and verification with EDS

Table 7 Drilling parameters and output variables

GFRP/Al drilling				GFRP		Al 2024	
Test	v_c (m/min)	Cooled air	F_t (N)	$F_{t,comp}$ (N)	F_{da}	R_a (µm)	t_{metal} (µm)
OTM 1	220	No	99.3	25.39	1.103	3.52	16.3
OTM 2	220	Yes	106.4	27.02	1.093	4.16	20.4
OTM 3	40	Yes	104.8	36.78	1.055	1.53	12.5
OTM 4	40	No	93.8	35.53	1.094	1.10	10.5

other studies [30, 39]. The thrust forces developed during the Al plate drilling were higher than those produced in the GFRP plate for all tested conditions. Higher cutting speeds provided a significant reduction of $F_{t,comp}$.

OTM 1 (higher v_c without cooled air) presented the highest adjusted delamination factor ($F_{da} = 1.103$) against slightly smaller values ($F_{da} = 1.093$) observed for OTM 2 (higher v_c with cooled air). More significant differences were observed between OTM 3 ($F_{da} = 1.055$) and OTM 4 ($F_{da} = 1.094$): tests performed with the lower cutting speed showed a significant improvement with cooled compressed air. In general, applying cooled air for both v_c positively influenced the F_{da} reduction, which agrees with other studies [9, 35, 36]. In addition, the small effect of the cutting speed on the delamination indicates the feasibility of using higher cutting speeds without damaging the composite material. This aspect is evidenced when holes drilled with OTM 1 and OTM 4 are compared.

Regarding the hole-wall roughness, higher R_a values were observed with higher v_c, as expected (OTM 1 and OTM 2). The use of cooled compressed air resulted in higher R_a for both cutting speeds. The influence, however, was not as strong as presented by the cutting speed. The increase in hole-wall roughness with the use of lubricating/cooling techniques was reported by [23].

Higher values of hole roundness deviation were observed with high v_c, as expected and indicated in the previous analyses. The highest roundness value (OTM 2) was observed with cooled air-assisted drilling, with a t_{metal} 25.2% higher than without cooled air (OTM 1). Similar results were observed for $v_c = 40$ m/min, in which the use of cooled air resulted in an increase of 19% in the hole roundness deviation. These effects could be attributed to process temperature, tool wear, lack of rigidity of the fastening system, among others [1, 20, 26]. In order to identify the best drilling condition for the GFRP/Al joint among those tested, a weight "2" was considered for delamination in the GFRP plate and weight "1" for thrust force, hole-wall roughness, and roundness deviation in the Al plate. With this criterion, the best drilling condition was defined as the OTM 3 ($v_c = 40$ m/min with cooled air). OTM 3 provided the lowest adjusted delamination factor ($F_{da} = 1.055$), the second lowest average roughness ($R_a = 1.53$ µm), and the second lowest hole roundness deviation ($t_{metal} = 12.5$ µm). The reduction of these values directly contributes to decreasing defects expected for composites and good levels of finish, which provide better fixation and adjustments [1, 3, 4].

Figure 13 shows the differences in the fracture of the GFRP fibers for the tested conditions. Considering OTM 1 (Fig. 13a), regular cuts and minor delamination on the hole's surface are observed in hole #3 ($v_c = 220$ m/min). Meanwhile, hole #10 (OTM 4, $v_c = 40$ m/min) shows regular fiber cuts and preservation of the polymer matrix. This situation points to low significant differences for both v_c in the drilling process of the GFRP/Al simple joint. Regarding cooled air application (Fig. 13b), regular cuts and smaller delamination are observed on the surface of hole #5 (OTM 2, higher v_c),

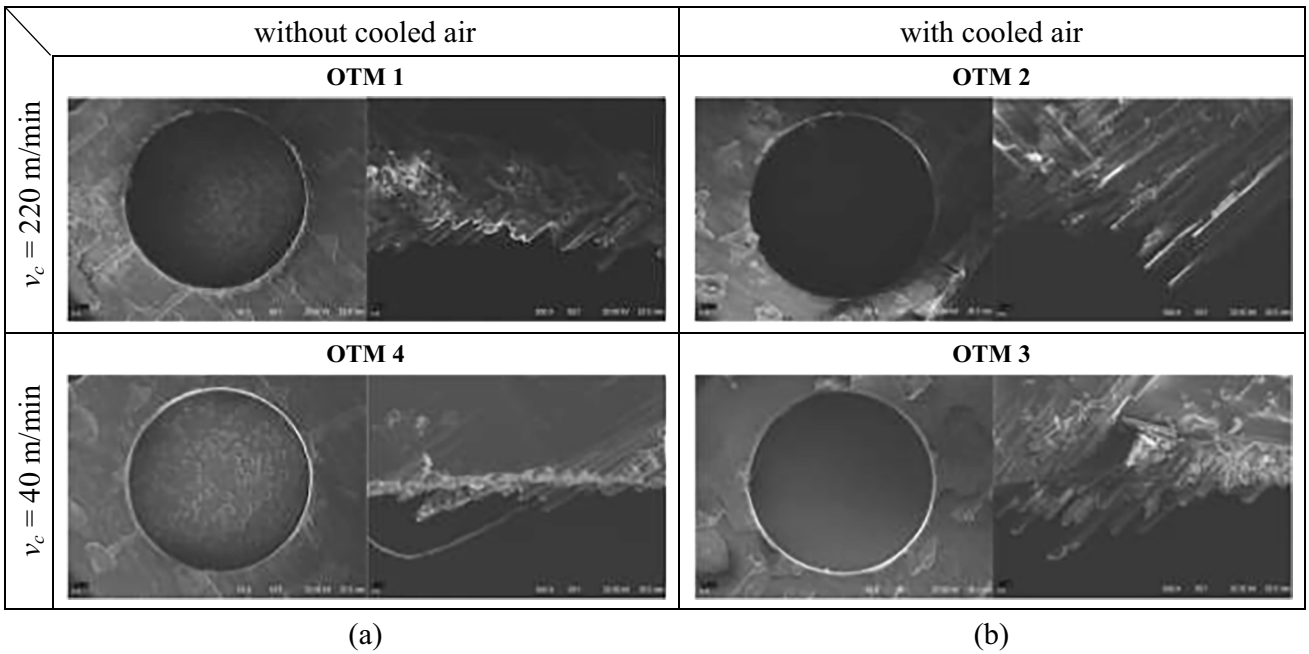

Fig. 13 SEM analysis of the holes at the exit of the GFRP. Comparison between: **a** hole #3 (OTM 1) and hole #10 (OTM 4); **b** hole #5 (OTM 2) and hole #7 (OTM 3)

and hole #7 (OTM 3, lower v_c) presents steady fiber cuts and preservation of the polymer matrix.

4 Conclusions

This work investigated the influence of cooled compressed air, associated with different cutting speeds and feed rates, on the drilling of hybrid composite-metal stacks (HCMS) with two different cutting tools. The study includes two stack types (simple and composed stacks), each tested with two different composite materials (GFRP and CFRP). The main conclusions are pointed out as follows.

- The different composite types (glass- or carbon-fiber-reinforced polymer) were significant for the defects observed in the process; the use of GFRP favored smaller delamination and hole-roundness errors.
- The joint type (simple or composite) strongly influenced the delamination of composite materials. Composed joints (Al/FRP/Al) significantly enhance roundness deviation and delamination.
- The cutting speed presented a significant influence on the adjusted delamination factor (F_{da}), with high v_c-inducing delamination.
- The use of high cutting speeds resulted in higher roundness deviations for the drilled holes in the aluminum plates. However, it did not affect the roundness of the holes in the CFRP. Even with the resulting decrease in the dimensional quality, an IT7 dimensional tolerance was achieved for all tested conditions, indicating that the feasibility of using HSC for production increases when geometric tolerances are required.
- The hole-wall roughness of the Al plate strongly depends on the cutting speed. Thus, the use of low v_c (40 m/min) is necessary when the surface finish of the drilled hole is required.
- Despite the increase of the thrust force and the negative influence expected on the delamination, the use of the high feed rate resulted in several improvements, including smaller roughness and roundness deviation of the holes in the Al plates. Despite the non-significant influence on F_{da}, some interactions of the feed rate did influence the delamination. The use of higher f allowed smaller F_{da} for the GFRP joints and holes drilled with the 86C drill.
- Additional tests performed for clarification of the effect of the cutting speed and cooled compressed air indicate that cooled air-assisted drilling with the 85C drill ($\sigma = 118°$), $v_c = 40$ m/min, and $f = 0.02$ mm/rev produce the best hole quality in GFRP/Al simple joint.
- The results of the additional tests indicate a stronger influence of cooled compressed air with lower cutting speed, with significantly smaller delamination for the drilling of GFRP simple joint.

Acknowledgements The authors thank the Sandvik Coromant for donating drills, the GEA-EESC-USP for the CFRP and GFRP plates, and the Embraer for the Al 2124 plate. The authors also thank the CIDEM-ISEP and INEGI-FEUP (Portugal) for the availability of equipment and systems, the CMM-UFRGS for valuable aid to image processing (MEV/EDS), and the Micromazza Co. for roundness error tests.

Author contribution Each author contributed to the research presented in this manuscript, approved the contents now presented, and agreed to the compliance with ethical standards.

Data availability The manuscript has no associated data in a data repository.

Materials availability The manuscript has no associated data in a data repository.

Declarations

Ethical approval The manuscript is original and has not been submitted for publication elsewhere (partially or in full). Also, the manuscript has not been submitted to more than one publication for simultaneous consideration.

Consent to participate Not applicable (this research did not involve human subjects).

Consent for publication All the authors consent to the manuscript's publication in the IJAMT should the article be accepted by the editor-in-chief upon completion of the refereeing process.

Competing interests The authors declare no competing interests.

References

1. Zitoune R, Krishnaraj V, Collombet F (2010) Study of drilling of composite material and aluminium stack. Compos Struct 92(5):1246–1255. https://doi.org/10.1016/j.compstruct.2009.10.010
2. Akhil KT, Shunmugesh K, Aravind S, Pramodkumar M (2017) Optimization of drilling characteristics using grey relational analysis (GRA) in glass fiber reinforced polymer (GFRP). Mater Today Proc 4:1812–1819. https://doi.org/10.1016/j.matpr.2017.02.024
3. Xu J, El Mansori M (2016) Experimental study on drilling mechanisms and strategies of hybrid CFRP/Ti stacks. Compos Struct 157:461–482. https://doi.org/10.1016/j.compstruct.2016.07.025
4. Lazar M-B, Xirouchakis P (2011) Experimental analysis of drilling fiber reinforced composites. Int J Mach Tools Manuf 51:937–946. https://doi.org/10.1016/j.ijmachtools.2011.08.009
5. Ho-Cheng H, Dharan CKH (1990) Delamination during drilling in composite laminates. J Manuf Sci Eng 112(3):236–239. https://doi.org/10.1115/1.2899580
6. Davim JP, Rubio JC, Abrao AM (2007) A novel approach based on digital image analysis to evaluate the delamination factor after drilling composite laminates. Compos Sci Technol 67(9):1939–1945. https://doi.org/10.1016/J.compscitech.2006.10.009

7. Gaitonde VN, Karnik SR, Rubio JC, Correia AE, Abrão AM, Davim JP (2008) Analysis of parametric influence on delamination in high-speed drilling of carbon fiber reinforced plastic composites. J Mater Process Technol 203(1–3):431–438. https://doi.org/10.1016/j.jmatprotec.2007.10.050
8. Khashaba UA, El-Sonbaty IA, Selmy AI, Megahed AA (2010) Machinability analysis in drilling woven GFR/epoxy composites: part I – effect of machining parameters. Compos Part A Appl Sci Manuf 41(3):391–400. https://doi.org/10.1016/j.compositesa.2009.11.006
9. Joshi S, Rawat K, Balan ASS (2018) A novel approach to predict the delamination factor for dry and cryogenic drilling of CFRP. J Mater Process Technol 262:521–531. https://doi.org/10.1016/j.jmatprotec.2018.07.026
10. Devitte C, Souza GSC, Souza AJ, Tita V (2021) Optimization for drilling process of metal-composite aeronautical structures. Sci Eng Compos Mater 28(1):264–275. https://doi.org/10.1515/secm-2021-0027
11. Srinivasan T, Palanikumar K, Rajagopal K, Latha B (2017) Optimization of delamination factor in drilling GFR–polypropylene composites. Mater Manuf Process 32(2):226–233. https://doi.org/10.1080/10426914.2016.1151038
12. Albuquerque VHC, Tavares JMRS, Durão LMP (2010) Evaluation of delamination damage on composite plates using an artificial neural network for the radiographic image analysis. J Compos Mater 44(9):1139–1159. https://doi.org/10.1177/0021998309351244
13. Shyha IS, Aspinwall DK, Soo SL, Bradley S (2009) Drill geometry and operating effects when cutting small diameter holes in CFRP. Int J Mach Tools Manuf 49(12–13):1008–1014. https://doi.org/10.1016/j.ijmachtools.2009.05.009
14. Kumar D, Sing KK (2017) Experimental analysis of delamination, thrust force and surface roughness on drilling of glass fibre reinforced polymer composites material using different drills. Mater Today Proc 4(8):7618–7627. https://doi.org/10.1016/j.matpr.2017.07.095
15. Durão LMP, Gonçalves DJS, Tavares JMRS, Albuquerque VHC, Marques AT (2012) Comparative analysis of drills for composite laminates. J Compos Mater 46(14):1649–1659. https://doi.org/10.1177/0021998311421690
16. Zitoune R, Krishnaraj V, Almabouacif BS, Collombet F, Sima M, Jolin A (2012) Influence of machining parameters and new nano-coated tool on drilling performance of CFRP/aluminium sandwich. Compos Part B Eng 43(3):1480–1488. https://doi.org/10.1016/j.compositesb.2011.08.054
17. Zhang L, Liu Z, Tian W, Liao W (2015) Experimental studies on the performance of different structure tools in drilling CFRP/Al alloy stacks. Int J Adv Manuf Technol 81:241–251. https://doi.org/10.1007/s00170-015-6955-z
18. Isbilir O, Ghassemieh E (2013) Comparative study of tool life and hole quality in drilling of CFRP/titanium stack using coated carbide drill. Mach Sci Technol 17:380–409. https://doi.org/10.1080/10910344.2013.806098
19. Velaga M, Cadambi RM (2017) Drilling of GFRP composites for minimising delamination effect. Mater Today Proc 4(10):11229–11236. https://doi.org/10.1016/j.matpr.2017.09.044
20. D'Orazio A, El Mehtedi M, Forcellese A, Nardinocchi A, Simoncini M (2017) Tool wear and hole quality in drilling of CFRP/AA7075 stacks with DLC and nanocomposite TiAlN coated tools. J Manuf Process 30:582–592. https://doi.org/10.1016/j.jmapro.2017.10.019
21. Ko SL, Lee JK (2001) Analysis of burr formation in drilling with a new-concept drill. J Mater Process Technol 113(1–3):392–398. https://doi.org/10.1016/S0924-0136(01)00717-8
22. Ko SL, Chang JE, Yang GE (2003) Burr minimizing scheme in drilling. J Mater Process Technol 140(1–3):237–242. https://doi.org/10.1016/S0924-0136(03)00719-2
23. Shyha IS, Soo SL, Aspinwall DK, Bradley S, Perry R, Harden P, Dawson S (2011) Hole quality assessment following drilling of metallic-composite stacks. Int J Mach Tools Manuf 51(7–8):569–578. https://doi.org/10.1016/j.ijmachtools.2011.04.007
24. Fu R, Jia Z, Wang F, Jin Y, Sun D, Yang L, Cheng D (2018) Drill-exit temperature characteristics in drilling of UD and MD CFRP composites based on infrared thermography. Int J Mach Tools Manuf 135:24–37. https://doi.org/10.1016/j.ijmachtools.2018.08.002
25. Peña B, Aramendi G, Rivero A, De Lacalle LNL (2005) Monitoring of drilling for burr detection using spindle torque. Int J Mach Tools Manuf 45(14):1614–1621. https://doi.org/10.1016/j.ijmachtools.2005.02.006
26. Qi Z, Ge E, Yang J, Li F, Jin S (2021) Influence mechanism of multi-factor on the diameter of the stepped hole in the drilling of CFRP/Ti stacks. Int J Adv Manuf Technol 113:923–933. https://doi.org/10.1007/s00170-021-06678-3
27. Ben W, Hang G, Quan W, Maoqing W, Sonpeng Z (2012) Influence of cutting heat on quality of drilling of carbon/epoxy composites. Mater Manuf Process 27(9):968–972. https://doi.org/10.1080/10426914.2011.610079
28. Merino-Pérez JL, Royer R, Merson E, Lockwood A, Ayvar-Soberanis S, Marshall MB (2016) Influence of workpiece constituents and cutting speed on the cutting forces developed in the conventional drilling of CFRP composites. Compos Struct 140:621–629. https://doi.org/10.1016/j.compstruct.2016.01.008
29. Merino-Pérez JL, Royer R, Ayvar-Soberanis S, Merson E, Hodzic A (2015) On the temperatures developed in CFRP drilling using uncoated WC-Co tools part I: workpiece constituents, cutting speed and heat dissipation. Compos Struct 123:161–168. https://doi.org/10.1016/j.compstruct.2014.12.033
30. Wang C-Y, Chen Y-H, An Q-L, Cai X-J, Ming W-W, Chen M (2015) Drilling temperature and hole quality in drilling of CFRP/aluminum stacks using diamond coated drill. Int J Precis Eng 16(8):1689–1697. https://doi.org/10.1007/s12541-015-0222-y
31. Eiamsa-Arda S, Promvonge P (2008) Review of Ranque-Hilsch effects in vortex tubes. Renew Sustain Energy Rev 12(7):1822–1842. https://doi.org/10.1016/j.rser.2007.03.006
32. Krishnaraj V, Prabukarthi A, Ramanathan A, Elanghovan N, Kumar MS, Zitoune R, Davim JP (2012) Optimization of machining parameters at high speed drilling of carbon fiber reinforced plastic (CFRP) laminates. Compos Part B Eng 43(4):1791–1799. https://doi.org/10.1016/j.compositesb.2012.01.007
33. Kuo CL, Soo SL, Aspinwall DK, Thomas W, Bradley S, Pearson D, M'Saoubi R, Leahy W (2014) The effect of cutting speed and feed rate on hole surface integrity in single-shot drilling of metallic-composite stacks. Procedia CIRP 13:405–410. https://doi.org/10.1016/j.procir.2014.04.069
34. Rezende BA, Silveira ML, Vieira LMG, Abrão AM, Faria PE, Rubio JCC (2016) Investigation on the effect of drill geometry and pilot holes on thrust force and burr height when drilling an aluminium/PE sandwich material. Materials (Basel) 9(9):774. https://doi.org/10.3390/ma9090774
35. Abish J, Samal P, Narenther MS, Kannan C, Balan ASS (2018) Assessment of drilling-induced damage in CFRP under chilled air

environment. Mater Manuf Process 33(12):1361–1368. https://doi.org/10.1080/10426914.2017.1415452
36. Hou G, Qiu J, Zhang K, Cao S, Cheng H, Luo B, Cheng Y (2020) Comparative tool wear and hole quality investigation in drilling of aerospace grade T800 CFRP using different external cooling lubricants. Int J Adv Manuf Technol 106:937–951. https://doi.org/10.1007/s00170-019-04554-9
37. Hoffmann N, Souza GSC, Souza AJ, Tita V (2021) Delamination and hole-wall roughness evaluation in air-cooled drilling of carbon fiber-reinforced polymer. J Compos Mater 55(23):3161–3174. https://doi.org/10.1177/00219983211009281
38. Trent EM, Wright PK (2000) Metal cutting. Butterworth-Heinemann, New York. https://www.sciencedirect.com/book/9780750670692/metal-cutting
39. Montoya M, Calamaz M, Gehin D, Girot F (2013) Evaluation of the performance of coated and uncoated carbide tools in drilling thick CFRP/aluminium alloy stacks. Int J Adv Manuf Technol 68:2111–2120. https://doi.org/10.1007/s00170-013-4817-0
40. Giasin K, Ayvar-Soberanis S (2016) Evaluation of workpiece temperature during drilling of GLARE fiber metal laminates using infrared techniques: effect of cutting parameters, fiber orientation and spray mist application. Materials (Basel) 9(8):622. https://doi.org/10.3390/ma9080622